

# Structural and Electrical Properties of Solid State Rechargeable LATP-Based Li-Ion Batteries Using $\text{LiMn}_2\text{O}_4$ as Cathode and Anode

H. M. Hashem\* and A. A. Zaki

Department of Physics, Faculty of Science, Helwan University,  
Cairo, Egypt

\* Corresponding author email: [hany\\_m\\_hashem@yahoo.com](mailto:hany_m_hashem@yahoo.com)

*The Battery was fabricated as metal/cathode/electrolyte/anode/metal.  $\text{Li}_{1.3}\text{Al}_{0.3}\text{Ti}_{1.7}(\text{PO}_4)_3$  based on NASICON framework (LATP) was used as the solid electrolyte with high ionic conductivity. The  $\text{LiMn}_2\text{O}_4$  thin film, which was used as cathode as well as anode electrode, was prepared by spray pyrolysis technique. Structural characteristics, using X-ray diffraction, showed that the best quality  $\text{LiMn}_2\text{O}_4$  film is obtained at substrate temperature of  $500^\circ\text{C}$  and flow rate of  $15\text{ L/min}$  with annealing at  $500^\circ\text{C}$  for  $10\text{ hr}$ . The electrical investigations were carried out using potentiostatic measurements and the performance by charge-discharge test as well as Ragone plot. The best performance (high power and high energy) was achieved for electrolyte of the maximum ionic conductivity prepared at temperature of  $950^\circ\text{C}$ .*

## 1. Introduction

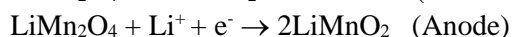
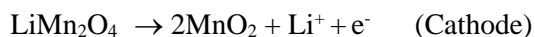
Over the past two decades, there has been a rise in the portable electronic device industry, which has fuelled the demand for high performance and reliable power sources. To support consumer needs, these electronic applications require rechargeable batteries that can offer long cycle and storage life, high volumetric and gravimetric energy densities and high power capabilities [1]. Lithium is the lightest metal and the most abundant on the earth. In the past two decades, Li-ion batteries have proved themselves the most advanced electrochemical power sources for portable electronic devices because of their high energy density, high power density, long cycle life, low cost and environmental friendliness including reduce of air pollution and global warming [2-5]. Several studies have been carried out for different electrolytes and electrodes but the complete answer for their influence is not yet clear. Also, the similarity between the features of electrochromic functional materials and rechargeable thin film batteries, concerning both the kinetics and mechanism of switching (charge/discharge cycles), was considered [6]. Sintered pellet of  $\text{Li}_{1.3}\text{Al}_{0.3}\text{Ti}_{1.7}(\text{PO}_4)_3$  (LATP) was

used as both solid electrolyte and substrate that will not increase the internal resistance [7]. However, enhancement of ionic conductivity of electrolyte is a major goal for a battery performance.

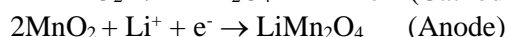
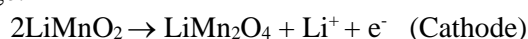
From the early 1990s onward, intensive efforts were devoted to the development of  $\text{LiMn}_2\text{O}_4$  material that has many advantages as electrodes for lithium-ion batteries [8 - 10]. Computational studies of spinel-structured of  $\text{LiMn}_2\text{O}_4$  indicate that Li-ion transport involves uniform migration via zig-zag type paths in all three dimensional pathways through its lattice [11, 12]. In addition, it shows small expansion and shrinkage of lattice constant during Li-ion insertion and extraction [13]. It can be also used as cathode and anode at the same times [7]. Lithium cells containing  $\text{LiMn}_2\text{O}_4$  can either be charged or discharged by cycling over a composition range of  $0 \leq x \leq 2$  in  $\text{Li}_x\text{Mn}_2\text{O}_4$  [14].

As  $\text{LiMn}_2\text{O}_4$  is used as electrode material and before any external load, the chemical potential (Fermi level) of the cathode and the anode is the same. The electrodes act as cathode or anode depending on the type of device and application. However, the general definition of “cathode is the source of electrons or an electron donor” can be considered. In the charging process, the Li-ion is extracted from the cathode to the electrolyte and an electron moves to the anode through the wire. Thus, the chemical potential of the cathode is changed due to phase change. At the same time, Li-ion from the electrolyte is inserted to the anode that gains electron from the cathode. Thus, the chemical potential of the anode is also changed due to the change of the phase. This charge/discharge mechanism is illustrated by the following equations:

Charge:



Discharge:



The goal of the work is the investigation of the constituents of the rechargeable all solid state Li-ion batteries in order to enhance their performance. This has to be achieved by investigation of LATP as the solid electrolyte by study the effect of preparation conditions on its structure characteristics (phase abundance and grain size) in correlation with its electric properties (electronic and ionic conductivity), which was given before in details by the authors [15]. The present work aims at optimization of the preparation parameters of  $\text{LiMn}_2\text{O}_4$  as the cathode and anode material. Then, study the combined effect of the LATP electrolyte and  $\text{LiMn}_2\text{O}_4$  electrodes on the performance of the device of the fabricated battery ( $\text{LiMn}_2\text{O}_4/\text{LATP}/\text{LiMn}_2\text{O}_4$ ). In this design, no extra substrate is used and only consists of two substances, which makes the fabrication of thin-film battery very simply [7].

## 2. Materials and Experimental Work

### 2.1. Electrodes

#### A) $\text{LiMn}_2\text{O}_4$ Precursor Solution

Stoichiometric amounts of lithium acetate and manganese acetate were dissolved in a small amount of deionized water with droplets of acetic acid while stirring and under heating at temperature  $150^\circ\text{C}$ . Then 2-methoxyethanol was added to adjust the viscosity and wetting property of the solution.  $\text{LiMn}_2\text{O}_4$  precursor solution of 0.2 mol/L was formed. Due to the volatile nature of lithium in the compound, an excess of 10% lithium [16] was added during the preparation of the precursor solution.

#### B) $\text{LiMn}_2\text{O}_4$ Thin Film

For fabricating of lithium-ion battery, a homemade low cost spray pyrolysis setup was used to prepare the  $\text{LiMn}_2\text{O}_4$  thin film cathode and anode material. This method has the advantage of stoichiometry control of the high quality product. The effect of the substrate temperature, flow rate and annealing on the phase formation as well as microstructure of the thin film were examined.

The precursor solution was sprayed onto glass substrate at different flow rates in the range from 10 to 20 L/min and temperatures of the substrate from  $320$  to  $500^\circ\text{C}$ . A rotating substrate holder and spray nozzle were used for spraying the aerosol uniformly on the pre-heated substrate through gravity feeding mechanism with the distance between the substrate and spray nozzle 40 cm. Pressurized air was the carrier gas and a pressure gauge was used to measure the pressure of the air. In order to avoid a decrease in substrate temperature during the deposition, many deposition cycles were used. Number of cycles were 20 cycles, interval between each successive cycles was 60 s and the spraying time was 60 s/cycle.

### 2.2. Battery Device

$\text{LiMn}_2\text{O}_4$  precursor solution was deposited by spray pyrolysis on both sides of the heated LATP pellets at  $500^\circ\text{C}$  in air as shown in Fig. (1). To make sure that the temperature is distributed homogeneously a special holder was designed. It was made from stainless steel and consists of six holes of 13 mm diameter and thickness of 3 mm. To make battery test, the device was coated with silver by thermal evaporation.

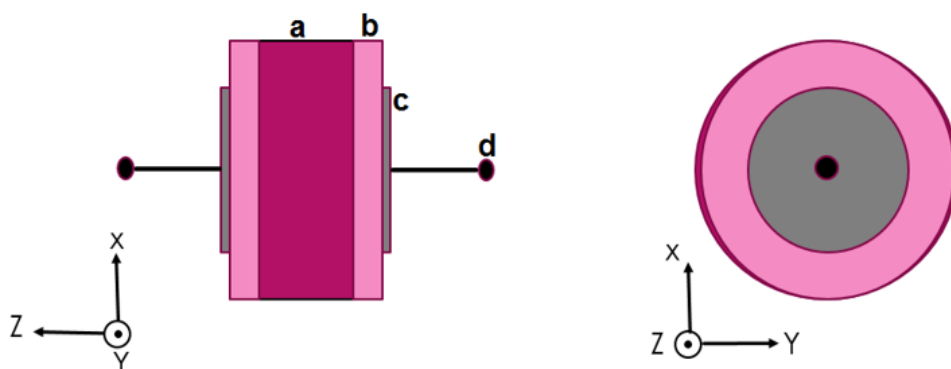


**Fig. (1):** Different 2D view of the battery: a) electrolyte, b) cathode, c) silver thin film, d) wire for electrochemical measurement.

## 2.3. Characterization

### 2.3.1. X-Ray Diffraction (XRD) Analysis

X-ray powder diffractometer was used for the structural analysis of the prepared films. The detector used in this work was a pixel 3D detector which is the most advanced two-dimensional photon counting device incorporating the latest in solid-state pixel technology. In this work, The XRD patterns of the prepared films onto glass substrate were collected at room temperature using Panalytical Empyrean diffractometer. The measurements were carried out using Ni-filtered  $\text{CuK}_\alpha$  radiation ( $\lambda = 1.540 \text{ \AA}$ ), at 45 kV and 30 mA. The  $2\theta$  range,  $10 \rightarrow 60^\circ$  was chosen to cover the main diffraction patterns of the prepared films. Step scanning size of  $0.1^\circ$ ,  $\Delta 2\theta$ , and counting time of 3 second per step were applied for the entire  $2\theta$ -range.

### 2.3.2. Battery Test

All the electrical studies and the battery tests were carried out using BioLogic potentiostat SP-150. To calculate the coulombic efficiency, charge/discharge cycles were performed applying a square wave biased voltage of amplitude  $\pm 1.5\text{V}$  with periodic time of 10 min.

A common way for comparing the performance of energy storage devices is to use the Ragone plot, which is a relation between the specific energy and specific power. In such plots, one performance attribute on the first axis is related to another performance attribute on the second axis. The specific form of the Ragone curve depends on the internal loss at high power and the leakage at low power of the energy saving devices. The Ragone plot was carried out by the constant power technique available with EC-Lab software in the Bio-Logic potentiostat, that is applied in a Li-ion battery test. The discharge time and the energy at constant power can be calculated from this plot.

### 3. Results and Discussion

#### 3.1. Electrodes

In order to optimize the preparation conditions, different substrate temperatures and different flow rates were considered with and without annealing. The X-ray diffractograms of the  $\text{LiMn}_2\text{O}_4$  electrodes that were prepared with spray pyrolysis at different substrate temperatures of 450 and 500 °C, but with constant flow rate of 10 L/min, were depicted in Fig. (2). No  $\text{LiMn}_2\text{O}_4$  phase was formed up to substrate temperature of 450°C; it starts to exist at temperature of 500 °C. With further annealing of the prepared film at 500 °C for 10 hr, the observed peaks became sharper, indicating a better crystallinity of the formed  $\text{LiMn}_2\text{O}_4$  phase.

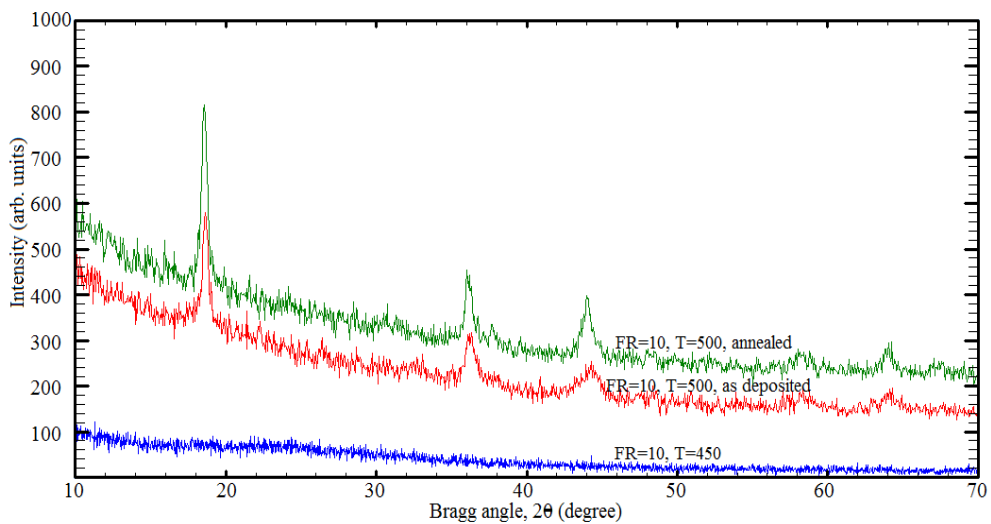


**Fig. (2):** XRD patterns of  $\text{LiMn}_2\text{O}_4$  thin film prepared by spray pyrolysis at different preparation temperatures.

In order to complete the optimization, constant substrate temperature of 500°C with annealing but different flow rates were investigated. The diffractograms of the prepared electrolytes are depicted in Fig. (3). Highest intensity, i.e. larger amount of material, and lower broadening, i.e. higher crystallinity, were observed in case of electrode prepared with flow rate =15 L/min. When the flow rate of air was 10 L/min, the quantity of  $\text{LiMn}_2\text{O}_4$  precursor solution was less than that at higher flow rates. On the other hand, when the flow rate is increased than 10 L/min, the substrate temperature descends, which decreases the crystallinity of  $\text{LiMn}_2\text{O}_4$  phase. Thus, the optimum conditions of  $\text{LiMn}_2\text{O}_4$  preparation is substrate temperature = 500°C and flow rate = 15 L/min, which were used in the fabrication of the device (battery).

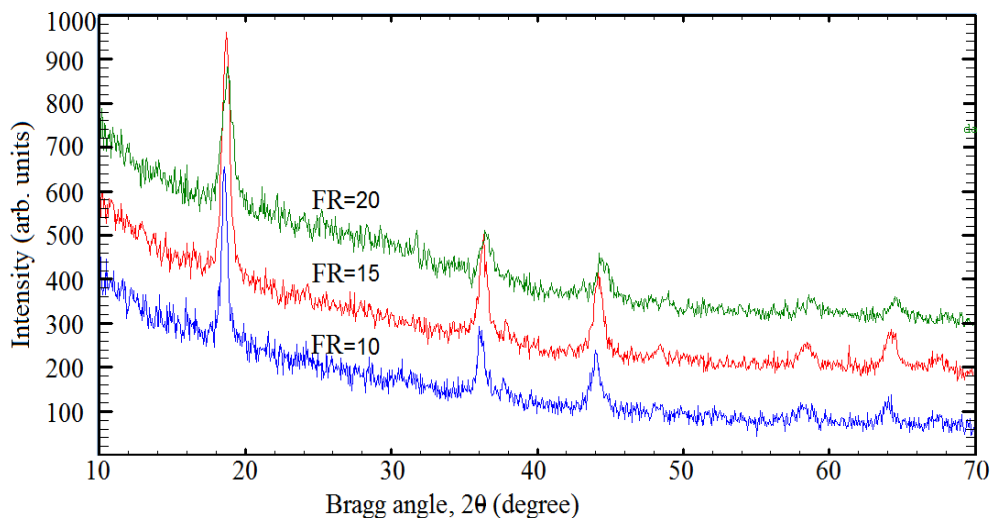


**Fig. (3):** XRD patterns of  $\text{LiMn}_2\text{O}_4$  thin film prepared by spray pyrolysis at different flow rates (L/min).

### 3.2. Electrolyte

The structure study of electrolyte prepared at different temperatures is illustrated in 2D contour plot of X-ray diffractograms as depicted in Fig. (4). In addition to LATP phase,  $\text{TiP}_2\text{O}_7$  one is also identified. At  $1000^\circ\text{C}$ , mainly a single phase of LATP is present. The quantitative analyses of both the phase concentration and grain size of LATP were investigated using Rietveld method. A plot of the final refinement for sample prepared at  $950^\circ\text{C}$  is depicted in Fig. (5), as a representative sample. The calculated LATP concentration and its grain size were given in Table (1). The LATP phase formation and grain size variation are sketched in Fig. (6) based on the refinement X-ray data. Depending on these microstructure characteristics, the behaviour of electric properties can be discussed. Although, electrolyte that prepared at  $950^\circ\text{C}$  has only 85% LATP, it shows the maximum ionic conductivity as measured by impedance spectroscopy (Nequest plot). This because the sample has connected grains with the largest size. Thus, high abundant of LATP with large connected grains is the required combination for high ionic conductivity.

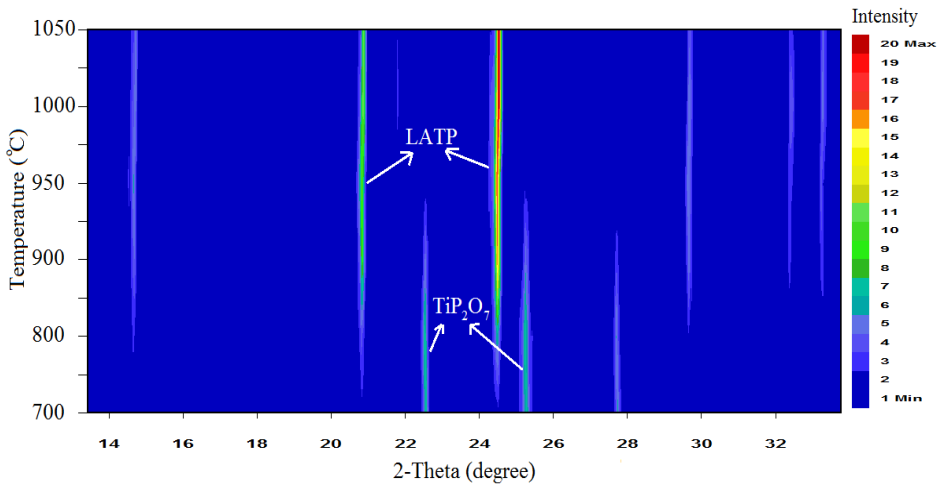


**Fig. (4):** 2D contour plot of X-ray diffractograms of electrolyte prepared at different temperatures.

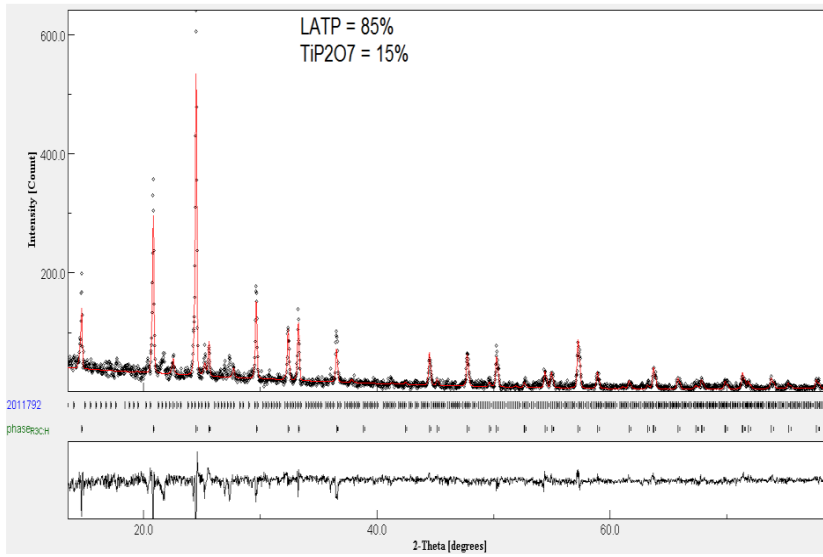


**Fig. (5):** Rietveld plot (dots are the experimental result, continues line is the refinement result and the difference in the lower part).

**Table 1.** LATP concentration and grain size.

Temperature (°C)	Concentration (wt. %)	Grain size (nm)
700	3	449
800	22	399
900	60	459
950	85	755
1000	95	622
1050	85	558

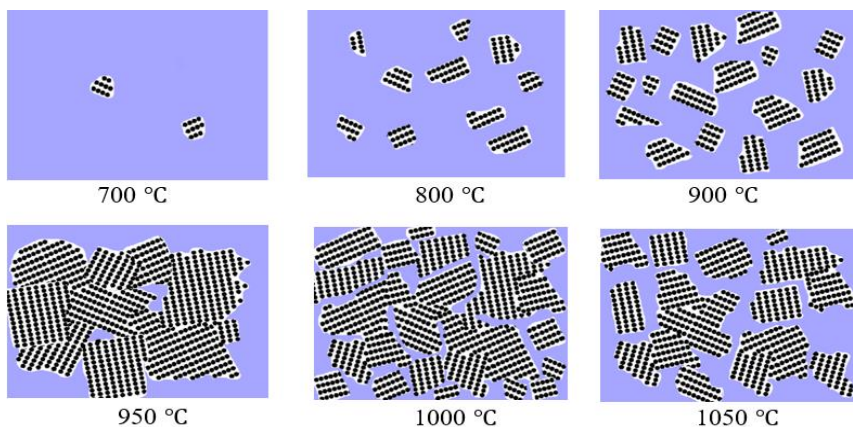


**Fig. (6):** Sketch of phase formation and grain size variation of LATP electrolyte with preparation temperatures.

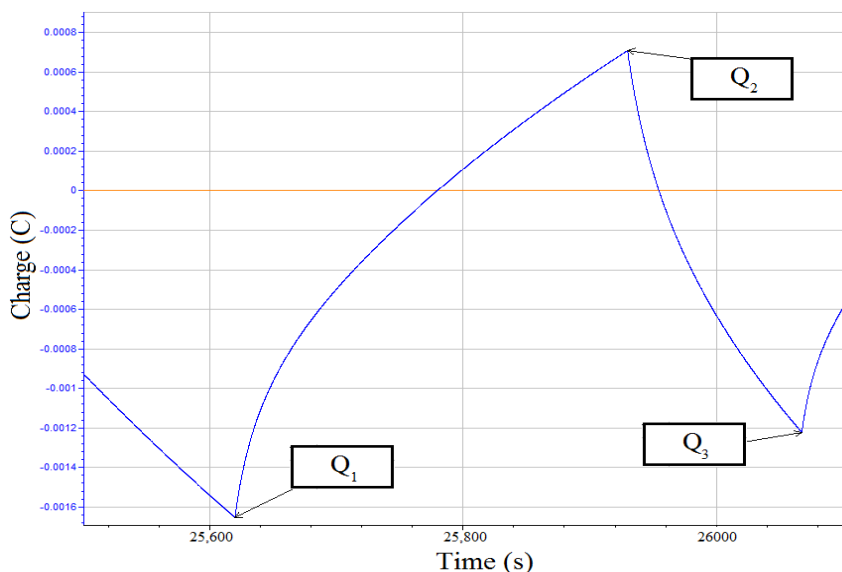
### 3.3. Battery Performance

The batteries were fabricated with electrolyte of LATP concentration in the range of  $\geq 22\%$  to 95% according to the intensive study published by the authors [15] and the  $\text{LiMn}_2\text{O}_4$  electrode of optimum preparation conditions. The performance of the batteries were then investigated to specify the best preparation temperature of the electrolyte.

#### (A) Efficiency

A typical charge-discharge curve of the batteries is illustrated in Fig. (7). The coulombic efficiency was calculated by the following equation:

$$\text{Efficiency} = Q_{\text{out}}/Q_{\text{in}} = (Q_2 - Q_3) / (Q_2 - Q_1)$$

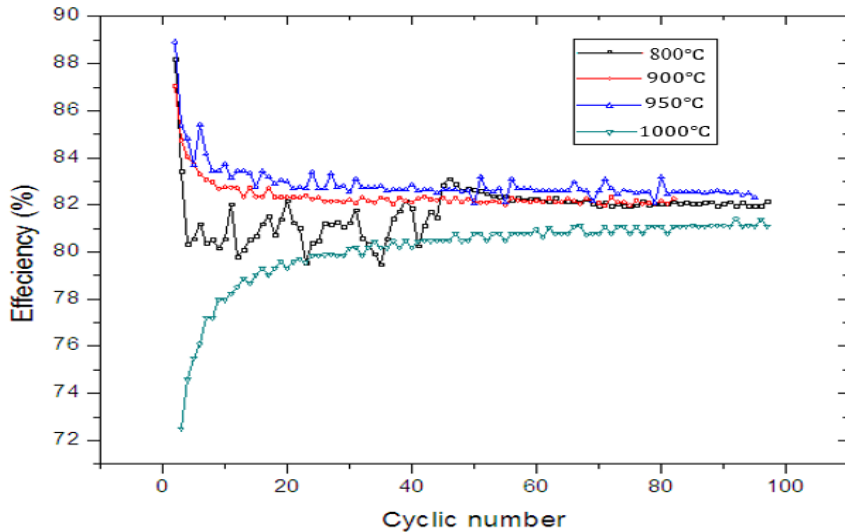


where  $Q_{\text{out}}$  is the output charge and  $Q_{\text{in}}$  is the input charge.

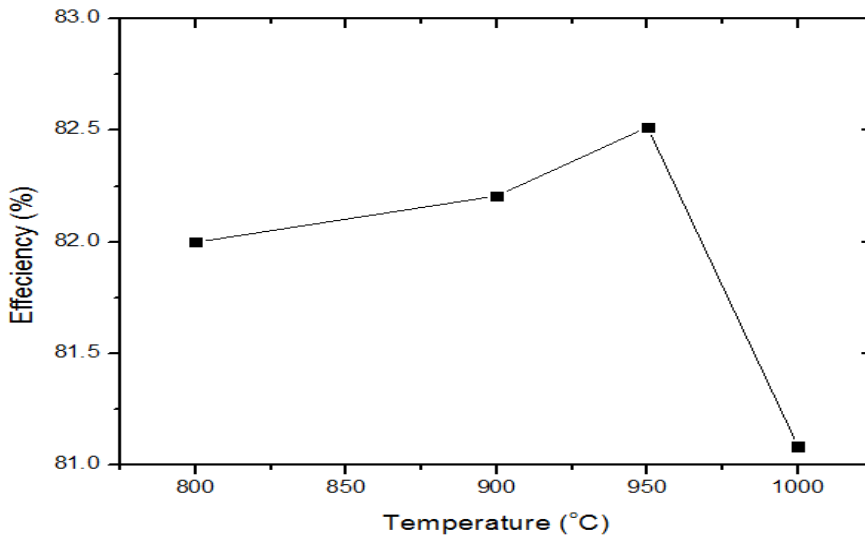


**Fig. (7):** Schematic of charge-discharge curve.

From the charge-discharge curves, the efficiency was calculated and represented as a function of cyclic number in Fig. (8). At first, the efficiency changes with cyclic number up to about 40 cycle, then a stable value is obtained. The efficiency of the prepared batteries after stability is illustrated in Fig. (9), as a function of preparation temperature. These efficiency values are accepted and are found within the values given in literature [7]. Generally, it is found that the preparation temperature has no appreciable effect on the coulombic efficiency up to 900°C. However, it can be observed that the temperature of 950°C provides the maximum value. Therefore, another test is required to identify more clearly the optimum temperature for better performance. Thus, Ragone plot was considered.

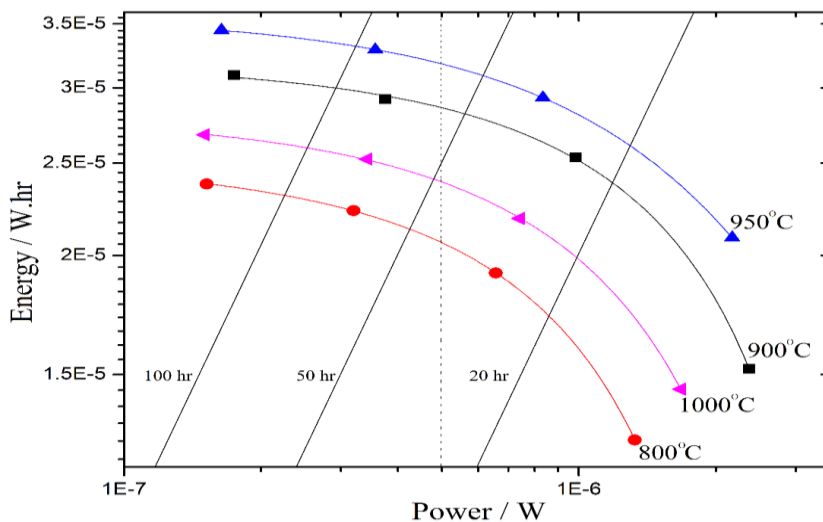


**Fig. (8):** Coulombic efficiency vs. cycle number for batteries of different preparation temperatures.



**Fig. (9):** Batteries efficiency after stability as a function of preparation temperatures.**(B) Ragone Plot**

Battery can be made to perform as an energy cell that stores a large amount of energy or a power cell that is capable to deliver high load current. Thus, batteries are characterized by the “energy” and the “power” being available [17]. The relationship between energy (E) and power (P) of battery can be best represented in Ragone plot, E(P). In logarithmic scale, it displays a performance profile of high and low values for discharge power and energy. The plot provides the available energy of a battery for a constant active power request as well as the characteristic time of an application. The optimum working region is the part of the curve where both energy and power are high. So that, it is a good presentation for performance comparison of various energy-storing devices. Ragone plots for the batteries (LiMn<sub>2</sub>O<sub>4</sub>/LATP/LiMn<sub>2</sub>O<sub>4</sub>) with electrolyte prepared at different temperatures are depicted in Fig. (10). Since the batteries are similar in sizes, shapes and weights, the plots are shown in energy and power, not in specific energy and specific power.

**Fig. (10):** Ragone plot for batteries with different preparation temperature of the electrolyte.

The available energy decreases substantially when drawing high power. This is mainly due to power loss and, hence, the significant voltage drop when drawing high currents. Consider the available energy for a constant power say  $4 \times 10^{-7}$  W (vertical dotted line in Fig. 12), it is clearly shown that the battery of an electrolyte prepared at 950°C provides the highest energy. On the other hand, consider the available energy for a constant time of certain application, say 50 hr, it is also shown that a battery of electrolyte prepared at 950°C provides the largest power during this time. This is also true at any longer or shorter time. The

discharge times at a fixed power of  $4 \times 10^{-7}$  W of the fabricated batteries of electrolyte prepared at 950 °C showed the longest time.

### Conclusions

The preparation parameters of all-solid state Li-ion batteries with the best performance are successfully achieved by the charge discharge test and Ragone plot investigations. The optimum conditions for the preparation of  $\text{LiMn}_2\text{O}_4$  electrodes (cathode/anode) by spray pyrolysis technique is flow rate of 15 L/min and substrate temperature of 500°C in addition to annealing at 500°C for 10 hr. This type of electrodes is recommended, where only two types of substances are used that makes the fabrication of a battery simpler. Electrolyte of the maximum electronic conductivity (high abundant of LATP with large connected grains) that was prepared at temperature of 950°C provides both the highest efficiency and optimal performance (high power and high energy) among all prepared battery devices.

### References

- [1] M. Armand, J.M. Tarascon, *Nature*, 451 (2008) 652-657.
- [2] E. Peled, *J. Electrochem. Soc.*, 126 (1979) 2047-2051.
- [3] J.M. Tarascon, M. Armand, *Issues and challenges facing rechargeable lithium batteries*, *Nature*, 414 (2001) 359-367.
- [4] S. Bashash, S. J. Moura, J. C. Forman, H. K. Fathy, *J. Power Sources*, 196 (2011), 541-549.
- [5] C. Wadia, P. Albertus, V. Srinivasan, *J. Power Sources*, 196 (2011) 1593-1598.
- [6] K-H Heckner, A. Kraft, *Solid State Ionics*, 152–153 (2002) 899– 905.
- [7] X. M. Wu, J. L. Liu, R. X. Li, S. Chen, M. Y. Ma, 47 (2011) 917–922.
- [8] J. M. Tarascon, E. Wang, F. K. Shokoohi, W. R. McKinnon, S. Colson, *J. Electrochem Soc*, 138 (1991) 2859–2864.
- [9] D. Guyomard, J. M. Tarascon, *Solid State Ionics*, 69 (1994) 222-237.
- [10] B. Xu, Y. S. Meng, *J. Power Sources*, 195 (2010) 4971-4976.
- [11] M. Nakayama, M. Kaneko, M. Wakihara, *Phys. Chem. Chem. Phys.*, 14 (2012) 13963-13970.
- [12] M. S. Islam, C. A. J. Fisher, *Chem. Soc. Rev*, 43 (2014) 185-204.
- [13] K. Dokko, K. Hoshina, H. Nakano, K. Kanamura, *Journal of Power Sources*, 174 (2007) 1100–1103.
- [14] R. J. Gummow, A. de Kock, M. M. Thackeray, *Solid State Ionics*, 69 (1994) 59-67.
- [15] A. A. Zaki, H. M. Hashem, S. Soltan, A. Abd El-Mongy and A. A. Ramadan, *International Journal of Current Research*, 8 (2016), 28385-28388.
- [16] A. Subramania, S. N. Karthick, N. Angayarkanni, *Thin Solid Films*, 516 (2008) 8295–8298.
- [17] C. Thomas, W. Martin, *Journal of Power Sources*, 91 (2000) 210-216.



### **Figure captions**

**Fig. 1.** Different 2D view of the battery: a) electrolyte, b) cathode, c) silver thin film, d) wire for electrochemical measurement.

**Fig. 2.** XRD patterns of  $\text{LiMn}_2\text{O}_4$  thin film prepared by spray pyrolysis at different preparation temperatures.

**Fig. 3.** XRD patterns of  $\text{LiMn}_2\text{O}_4$  thin film prepared by spray pyrolysis at different flow rates (L/min).

**Fig. 4.** 2D contour plot of X-ray diffractograms of electrolyte prepared at different temperatures.

**Fig. 5.** Rietveld plot (dots are the experimental result, continues line is the refinement result and the difference in the lower part).

**Fig. 6.** Sketch of phase formation and grain size variation of LATP electrolyte with preparation temperatures.

**Fig. 7.** Schematic of charge-discharge curve.

**Fig. 8.** Coulombic efficiency vs. cycle number for batteries of different preparation temperatures.

**Fig. 9.** Batteries efficiency after stability as a function of preparation temperatures.

**Fig. 10.** Ragone plot for batteries with different preparation temperature of the electrolyte.